Calculation of the magnetic properties of Fe, Co and Ni with account taken of the real band structure and spin fluctuations

Calculation of the magnetic properties of Fe, Co and Ni with account taken of the real band structure and spin fluctuations

B I Reser

Institute of Metal Physics, Ural Branch of the Russian Academy of Sciences, 620219
Ekaterinburg, GSP-170, Russia

Abstract.   The method for calculation of the mean and local magnetic characteristics of ferro-
magnetic metals at finite temperatures, developed by the author and co-workers in previous papers
and based on using the real band structure and spin fluctuations, is applied to Fe, Co and Ni. The
initial parameters of the calculation are the electron density of states and the magnetic moment at
$T = 0$ for a specific metal. The magnetization, the Curie temperature, the local magnetic moment
and the uniform and local susceptibilities are calculated for ferromagnetic and paramagnetic states.
The results are in agreement with experimental data over a wide range of temperatures.

1. Introduction

It is well known that in the traditional Stoner theory of magnetism [1] the only source of
temperature dependence is the Fermi distribution function $f(\varepsilon) = [\exp((\varepsilon - \mu)/T) + 1]^{-1}$.
Since in metals $\mu/T \gg 1$, within the framework of this theory, the influence of temperature
is very weak and the observed temperature behaviour, in general, is not explained. Substantial
progress in the explanation of the temperature dependence of the magnetic properties of ferro-
magnetic metals has been observed only in recent years, and it is connected with taking account
of the electron spin-density fluctuations (see, e.g., [2, 3]). Unfortunately, even in the static
local approximation [4, 5] the spin-fluctuation theory (SFT) is very complicated and one has
to introduce a number of significant simplifications in performing actual calculations (see,
e.g., [4–11] and references therein). In particular, the initial density of states (DOS) is always
chosen in a simplified model form, and the Fermi distribution is replaced by a step function.

A simple method for calculation of magnetic characteristics of ferromagnetic metals at
finite temperatures, based on using the real band structure and spin fluctuations in the static local
approximation, was developed in [12]. However, in full accord also with the results of other
spin-fluctuation calculations, based on a static approximation, this method gives a temperature
dependence of the magnetization that is not in sufficient agreement with experimental data,
especially at low temperatures, gives a small effective moment in the Curie–Weiss law etc.
In this connection, in the paper [13], we extended our method to the case of dynamic non-
local fluctuations. This method is based on a self-consistent quadratic approximation to the
free energy of electrons in a random exchange field. The initial parameters of the calculation
are the DOS and the magnetic moment at $T = 0$ for a specific metal. In the present paper,
detailed quantitative calculations of the temperature dependence of the magnetic properties
of Fe, Co and Ni are made, using the first-principles DOS and various approximations of

SFT. A comparative investigation of the statics, dynamics and space correlation of the spin fluctuations in these metals is also given.

Note that in calculating the temperature dependence of the magnetic properties of Fe, Co and Ni, we use the rigorous SFT complemented by taking into account the real band structure. In a number of recent studies (see, e.g., [14–16]) the opposite approach is used: rigorous band calculations of Fe, Co and Ni are complemented by a simplified accounting for spin fluctuations. So, in the papers [14, 16] the weak-itinerant-ferromagnetism limit of the SFT [17, 18], which, strictly speaking, is appropriate only for metals with small magnetic moments and low T_C, is used. In the paper [15] the spin fluctuations (in the paramagnetic region) are taken into account by replacing the Weiss field with a generalized Onsager cavity field [19], which corresponds to taking explicit account of the short-range order. Thus, the epithet 'first-principles' in application to the SFT used in [15, 16] means only that the results are obtained on the basis of first-principles band calculations. As for taking account of spin fluctuations, this is done in the framework of approximate physical models. We emphasize that all of the above-mentioned calculations—both single-site [4–11] and long-wavelength ones [14–16]—are performed in the static approximation, i.e. in these calculations the spin fluctuations are treated classically.

Finally, in a recent paper [20] the magnetic properties of Ni were calculated rather successfully within the Stoner theory. However, in this calculation, the effective band structure obtained by hybridization of the spin-polarized and paramagnetic band structures was used. The equation for the effective-band-structure calculation incorporates both the experimentally observed temperature-dependent magnetization and the zero-temperature experimental value of the exchange splitting at the point L_3. Of course, in the approach of [20], the local magnetic moment at T_C vanishes, but whether this is so for Ni remains debatable (see, e.g., [21]), as does the assertion that the spin fluctuations in Ni have pronounced itinerant character.

A detailed comparison of our results with the results from references [14–16, 20] is given in subsection 3.4.

2. Method

Let us give the basic ideas of the method for calculation of the magnetic properties of ferromagnetic metals at finite temperatures developed in [12, 13] and present the final formulae essential for an understanding of the results of our investigation.

The pair interaction of electrons characterized by the interatomic electron repulsion constant u is replaced by the interaction of electrons with the exchange field $V \equiv (V_1, V_2, \ldots)$, $V_j = \boldsymbol{V}_j(\tau) \cdot \boldsymbol{\tau}$, fluctuating in space and in 'time' $\tau \in [0, 1/T]$, where j is the site number and the τ are the Pauli matrices. The free energy of the electrons in a fluctuating field is approximated with the quadratic form

$$F(V) = \sum_{qn\alpha} \Delta V_{qn}^{\alpha} (u^{-1} - \chi_{qn}^{\alpha}) \Delta V_{-q-n}^{\alpha} \tag{1}$$

where

$$\chi_{qn}^{\alpha} \equiv \chi_q^{\alpha}(\mathrm{i}\omega_n) = -\frac{N}{2} T \, \mathrm{Sp} \sum_{km} \langle G(V) \rangle_{km} \tau^{\alpha} \langle G(V) \rangle_{k-q,m-n} \tau^{\alpha} \tag{2}$$

is the spin susceptibility of non-interacting electrons (in units of $g^2 \mu_B^2/2$) and ΔV_{qn}^{α} is the fluctuation of the exchange field ($\alpha = x, y, z$) written down in the momentum–'frequency' ($q\omega_n$) representation. The Green function

$$G(V) = (z + \mu - H_0 - V)^{-1} \tag{3}$$

is written down in the $q\omega_n$ representation too. In formulae (1)–(3), z is the energetic variable, μ the chemical potential, H_0 the operator of the kinetic and potential energy of the electrons in the crystal field, $\omega_n = 2\pi nT$ the thermodynamic frequency, N the number of (degenerate) energy bands, Sp the sum of diagonal elements over the spin projection index $\sigma = \uparrow, \downarrow$ or ± 1 and the average is defined by the formulae

$$\langle \cdots \rangle = \int c(V) \cdots \, \mathrm{d}V \qquad c(V) = \exp(-F(V)/T) \int \exp(-F(V)/T) \, \mathrm{d}V. \tag{4}$$

In the single-site quasi-static scattering approximation, in the case of ferromagnets (and paramagnets), the mean single-site Green function $\langle G(V) \rangle_{ii} = g$ is independent of the site index i, is spin (σ) diagonal and is written as

$$g_\sigma(\varepsilon) = \int \frac{\nu(\varepsilon')}{\varepsilon - \sigma \langle V_z \rangle - \Delta\Sigma_\sigma(\varepsilon) - \varepsilon'} \, \mathrm{d}\varepsilon' \tag{5}$$

where $\nu(\varepsilon)$ is the non-magnetic DOS (per unit cell, band and spin) and $\Delta\Sigma_\sigma(\varepsilon)$ is the fluctuation contribution to the self-energy part. For the contribution $\Delta\Sigma_\sigma$, in the lowest order of field fluctuations we obtain the approximate formula

$$\Delta\Sigma_\sigma(\varepsilon) = \frac{g_\sigma^s(\varepsilon)\langle \Delta V_z^2 \rangle}{1 + 2\sigma \langle V_z \rangle g_\sigma^s(\varepsilon)} + 2g_\sigma^s(\varepsilon)\langle \Delta V_x^2 \rangle \tag{6}$$

where $g_\sigma^s(\varepsilon)$ is determined by expression (5) at $\Delta\Sigma_\sigma(\varepsilon) = 0$.

We are now faced with the problem of calculating the mean square of the fluctuations of the on-site exchange field ('fluctuations', for short):

$$\zeta^\alpha \equiv \langle \Delta V_\alpha^2 \rangle = \frac{1}{N_a} \sum_{qn} \langle |\Delta V_{qn}^\alpha|^2 \rangle \tag{7}$$

where N_a is the number of atoms (unit cells). Taking into account (4) and (1), for the temperature-dependent contribution to the sum over n we have

$$\sum_n{}' \langle |\Delta V_{qn}^\alpha|^2 \rangle = \frac{u}{2} \frac{2}{\pi} \int_0^\infty \frac{1}{\mathrm{e}^{\varepsilon/T} - 1} \, \mathrm{Im} \, \frac{1}{1 - u\chi_q^\alpha(\varepsilon + \mathrm{i}0)} \, \mathrm{d}\varepsilon. \tag{8}$$

We discard the temperature-independent terms, assuming that the zero-point fluctuations are already taken into account in the initial DOS $\nu(\varepsilon)$ calculated by the density-functional method and in the effective interaction constant u.

Since the Bose function is strongly localized near zero energy, it is sufficient to know the behaviour of the susceptibility $\chi_q(\varepsilon)$ for $\varepsilon \to 0$ only. Using an expansion of the complex function $\chi_q(\varepsilon)$ at small thermal energies, $\varepsilon \sim T$,

$$\chi_q(\varepsilon) = \chi_q(0) + \mathrm{i}\varphi_q\varepsilon \tag{9}$$

and the approximation

$$\frac{1}{\mathrm{e}^{\varepsilon/T} - 1} \simeq \begin{cases} T/\varepsilon & \varepsilon < \varepsilon_0 = (\pi^2/6)T \\ 0 & \varepsilon > \varepsilon_0 \end{cases} \tag{10}$$

for the Bose function, we calculate the integral in (8) analytically and obtain

$$\sum_n{}' \langle |\Delta V_{qn}^\alpha|^2 \rangle = \frac{uT}{2\lambda_q^\alpha} \frac{2}{\pi} \arctan \frac{u\varphi_q^\alpha \pi^2 T}{6\lambda_q^\alpha} \tag{11}$$

where

$$\lambda_q^\alpha = 1 - u\chi_q^\alpha(0). \tag{12}$$

The real functions λ_q^α and φ_q^α can be calculated using (2), but this calculation is too cumbersome to be rewarding. We take advantage of reasonable approximations. For the static susceptibility $\chi_q^\alpha(0)$ we use the approximation

$$\chi_q^\alpha(0) = \chi_0^\alpha(0) + B^\alpha q^2 \tag{13}$$

where the coefficient B^α is expressed in terms of the local susceptibility, which is the average over the wave vectors within the Brillouin zone (BZ):

$$\chi_L(0) = \frac{1}{N_a} \sum_q \chi_q(0) \equiv \overline{\chi}_q(0).$$

The substitution of (13) into (12) gives

$$\lambda_q^\alpha = \lambda_0^\alpha + (\lambda_L^\alpha - \lambda_0^\alpha) q^2 / \overline{q^2} \tag{14}$$

where

$$\lambda_0^\alpha = 1 - u\chi_0^\alpha(0) \qquad \lambda_L^\alpha = 1 - u\chi_L^\alpha(0). \tag{15}$$

Accordingly, we replace the function φ_q^α by its average value:

$$\overline{\varphi}_q^\alpha = \varphi_L^\alpha. \tag{16}$$

Converting the q-sum in (7) into an integral over the BZ, replaced by a sphere of the same volume for simplicity, and using (11), (14) and (16) we obtain

$$\zeta^\alpha = \frac{uT}{2\lambda_L^\alpha} \int_0^1 \frac{1}{a_\alpha^2 + b_\alpha^2 k^2} \frac{2}{\pi} \arctan \frac{c_\alpha}{a_\alpha^2 + b_\alpha^2 k^2} 3k^2 \, dk \qquad 0 < a_\alpha^2 < 1 \tag{17}$$

where

$$k = q/q_B$$
$$a_\alpha^2 = \lambda_0^\alpha/\lambda_L^\alpha \qquad b_\alpha^2 = (1 - a_\alpha^2)/\overline{q^2} q_B^2 \qquad c_\alpha = u\varphi_L^\alpha \pi^2 T/(6\lambda_L^\alpha)$$
$$\overline{q^2} = 0.6 q_B^2$$

and q_B is the radius of a sphere with the BZ volume.

Since, in the absence of magnetic anisotropy, any small external magnetic field causes rotation of the large spontaneous magnetization of the ferromagnet, i.e. the enhanced susceptibility $\tilde{\chi}_0^\alpha(0) = \chi_0^\alpha(0)/\lambda_0^\alpha$ diverges, we assume that $\lambda_0^\alpha = 0$ at $T < T_C$. In the paramagnetic region ($T > T_C$), the static uniform susceptibility $\chi_0^z(0) = \chi_0^x(0)$ is found by numerical differentiation of the spin moment ρ_z over the magnetic field h, with the mean field $\langle V_z \rangle$ kept fixed:

$$\chi_0^z(0) = -\frac{\partial \rho_z}{\partial h} \simeq -\frac{\rho_z(\langle V_z \rangle + h/2) - \rho_z(\langle V_z \rangle - h/2)}{h}. \tag{18}$$

Taking into account (2), for the local susceptibility we have

$$\chi_L^\alpha(z) = -\frac{N}{2\pi} \mathrm{Sp} \int \mathrm{Im}\, g(\varepsilon) \, \tau^\alpha [g(\varepsilon - z) + g(\varepsilon + z)] \tau^\alpha f(\varepsilon) \, d\varepsilon$$

whence

$$\chi_L^x(0) = -\frac{N}{\pi} \int \mathrm{Im}(g_\uparrow g_\downarrow) f \, d\varepsilon \qquad \varphi_L^x = \frac{N}{\pi} \int \mathrm{Im}\, g_\uparrow \, \mathrm{Im}\, g_\downarrow \left(-\frac{\partial f}{\partial \varepsilon}\right) d\varepsilon$$

$$\chi_L^z(0) = \frac{1}{4}(\chi_L^\uparrow(0) + \chi_L^\downarrow(0)) \qquad \chi_L^\sigma(0) = -\frac{2N}{\pi} \int \mathrm{Im}\, g_\sigma^2 \, f \, d\varepsilon \tag{19}$$

$$\varphi_L^z = \frac{1}{4}(\varphi_L^\uparrow + \varphi_L^\downarrow) \qquad \varphi_L^\sigma = \frac{2N}{\pi} \int (\mathrm{Im}\, g_\sigma)^2 \left(-\frac{\partial f}{\partial \varepsilon}\right) d\varepsilon.$$

At fixed values of the fluctuations ζ^α, the equations for the mean field $\langle V_z \rangle$ and chemical potential μ are solved:

$$\langle V_z \rangle = -u\rho_z \qquad \rho_z = (n_\uparrow - n_\downarrow)/2 \qquad n_e = n_\uparrow + n_\downarrow \tag{20}$$

where

$$n_\sigma = \frac{N}{\pi} \int \operatorname{Im} g_\sigma(\varepsilon) \, f(\varepsilon) \, \mathrm{d}\varepsilon \tag{21}$$

is the number of electrons with spin projection σ and n_e is the total number of d electrons.

At $\zeta^\alpha = 0$, equations (5), (20) and (21) turn into the mean-field-theory equations. This gives one an opportunity to find at $T = 0$ the effective constant u from a known magnetic moment (per atom) $m_0 = g\mu_B \rho_z(0)$; after that the equations (5), (6), (17)–(21) make up a closed system with respect to the four variables ζ^x, ζ^z, $\langle V_z \rangle$ and μ. In various approximations for the SFT, only formula (17) for the spin fluctuations is modified. In the static local approximation it takes the form

$$\zeta_{SL}^\alpha = \frac{uT}{2\lambda_L^\alpha} \tag{22}$$

while in the static non-local approximation it is

$$\zeta_{SN}^\alpha = \frac{uT}{2\lambda_L^\alpha} \int_0^1 \frac{1}{a_\alpha^2 + b_\alpha^2 k^2} 3k^2 \, \mathrm{d}k = \frac{uT}{2\lambda_L^\alpha} \frac{3}{b_\alpha^3} \left(b_\alpha - a_\alpha \arctan \frac{b_\alpha}{a_\alpha} \right) \tag{23}$$

and in the dynamic local approximation it is

$$\zeta_{DL}^\alpha = \frac{uT}{2\lambda_L^\alpha} \frac{2}{\pi} \arctan c_\alpha. \tag{24}$$

Solving the magnetic problem considered at a fixed temperature, we calculate the mean DOS $\nu_\sigma(\varepsilon) = \pi^{-1} \operatorname{Im} g_\sigma(\varepsilon)$, the magnetization $m = g\mu_B \rho_z$, the static uniform susceptibility $\tilde\chi_0 = \chi_0/(1 - u\chi_0)$, the local magnetic moment m_L, the longitudinal (T_1) and transverse (T_2) nuclear spin-relaxation times. Comparing the susceptibility $\tilde\chi_0$ in the paramagnetic region with the Curie–Weiss law $\chi = m_{eff}^2/(3(T - \Theta_C))$, we determine the value of the effective magnetic moment m_{eff} and the paramagnetic Curie temperature Θ_C. The local magnetic moment is calculated from the formulae

$$m_L(T)/m_0 = [(\langle V_z \rangle^2(T) + \langle (\Delta V)^2 \rangle - 3uT/2)/\langle V_z \rangle^2(0)]^{1/2} \tag{25}$$

$$m_L(T)/m_0 = [(\langle V_z \rangle^2(T) + \langle (\Delta V)^2 \rangle)/\langle V_z \rangle^2(0)]^{1/2} \tag{26}$$

which are obtained in the functional integral theory (see, e.g., [2]) in the static and dynamic approximations, respectively. The relaxation times are calculated from the formulae [22]

$$\frac{1}{T_1 T} = c \frac{2 \operatorname{Im} \tilde\chi_L^x(\varepsilon_0, T)}{\varepsilon_0} \qquad \frac{1}{T_2 T} = \frac{1}{2} \frac{1}{T_1 T} + c \frac{\operatorname{Im} \tilde\chi_L^z(\varepsilon_0, T)}{\varepsilon_0}$$

(c is a constant; $\varepsilon_0 \sim 10^{-4}$–$10^{-5}$ eV) which taking into account the expansion

$$\chi_L^\alpha(\varepsilon) = \chi_L^\alpha(0) + i\varphi_L^\alpha \varepsilon$$

take the forms

$$\frac{1}{T_1 T} = c \frac{2\varphi_L^x}{(1 - u\chi_L^x(0))^2} \qquad \frac{1}{T_2 T} = \frac{1}{2} \frac{1}{T_1 T} + c \frac{1}{4} \sum_\sigma \left(\frac{1 + u\chi_L^{\bar\sigma}(0)/2}{1 - u^2 \chi_L^\sigma(0)\chi_L^{\bar\sigma}(0)/4} \right)^2 \varphi_L^\sigma. \tag{27}$$

From here, in particular, for $u \to 0$, i.e. without allowing for enhancement, it follows that

$$\frac{1}{T_1^0 T} = c\, 2\varphi_L^x \qquad \frac{1}{T_2^0 T} = \frac{1}{2} \frac{1}{T_1^0 T} + c\varphi_L^z. \tag{28}$$

The details of the calculations of the magnetic characteristics were described in our papers [12, 13, 23]. In [23] we developed a general numerical method for calculation of the integrals, involving the Fermi function. A simple method for calculation of the integrals, involving the derivative of the Fermi function, is given in the appendix.

3. Results and discussion

3.1. Iron

As the initial DOS, we take that of non-magnetic iron, calculated in the local-density approx-imation (LDA) by the Korringa–Kohn–Rostoker (KKR) method with a self-consistent potential [24]. The extended 'tails' and the constant sp background were eliminated from this DOS, so that the area under the curve was equal to 10 (the number of d states per atom). This yields a d band of width $W = 7.42$ eV. Then the DOS was slightly smoothed out by convolution with the Lorentz function of half-width $\Gamma = 0.01W$ to remove non-physical sharp peaks, which always appear in energy band calculations entirely ignoring single-particle-state damping due to electron–electron scattering. The DOSs thus obtained, normalized to one state (per atom, band and spin), are shown in figure 1. The number of d electrons per atom is $n_e = 7.43$. The effective interaction constant u determined from an experimental value of the magnetic moment $m_0 = 2.217$ μ_B [25] was 1.08 eV.
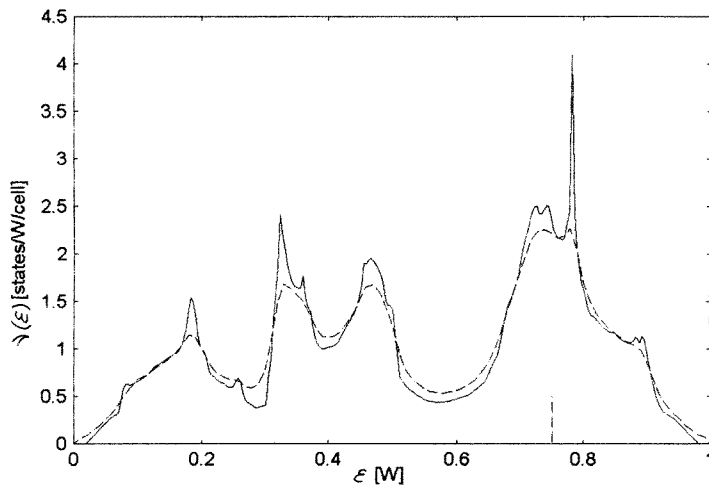

Figure 1. The DOS of the d band of non-magnetic iron, calculated by the KKR method with a self-consistent potential (——), and that smoothed out by convolution with the Lorentz function of half-width $\Gamma = 0.01$ (– – –). The energy ε and half-width Γ are in units of the bandwidth $W = 7.42$ eV. The vertical line indicates the position of the Fermi level ε_F.

The results of the calculation of the basic magnetic characteristics of iron in the mean-field theory and in various approximations of the SFT are represented in table 1 and figures 2–5. All of the characteristics are expressed in units of their experimental values given in table 2.

As can be seen from table 1, in the mean-field theory the temperature dependence of the magnetization is very weak and the calculated Curie temperature obtained is almost six times greater than the observed one.

In the SFT the situation is substantially different. Let us start from the static local approx-imation (SLA), in which the fluctuations are calculated from formula (22). In the SLA, as can be seen from figure 2, the Curie temperature is close to the experimentally observed one, $T_C = 1.28 T_C^{exp}$. However, a noticeable decrease of the magnetization, $\sim T$, is seen over a wide temperature interval (figure 2), which is due to the fact that spin fluctuations increase linearly with temperature. In general, the paramagnetic susceptibility follows the Curie–Weiss law, but the effective magnetic moment m_{eff} is only 0.66 of its experimental value. The paramagnetic

Table 1. The ferromagnetic (T_C) and paramagnetic (Θ_C) Curie temperatures, and the effective magnetic moment m_{eff} in the mean-field theory and in various approximations of the spin-fluctuation theory.

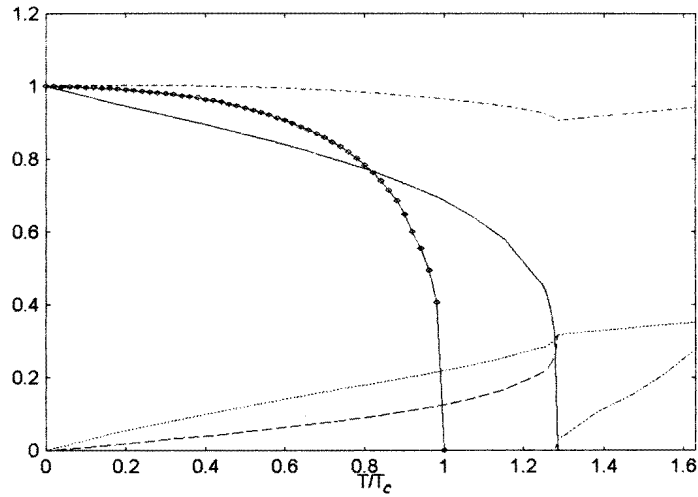| Metal	Magnetic characteristic	Mean-field theory	Spin-fluctuation theory			
			SLA	SNA	DLA	DNA
Fe	T_C/T_C^{exp}	5.84	1.28	0.76	2.45	1.49
	θ_C/T_C^{exp}	5.82	1.24	0.77	2.29	1.45
	m_{eff}/m_{eff}^{exp}	0.86	0.66	0.98	0.80	1.30
Co	T_C/T_C^{exp}	3.61	0.55	0.32	1.23	0.63
	θ_C/T_C^{exp}	3.60	0.54	0.34	1.22	0.68
	m_{eff}/m_{eff}^{exp}	0.84	0.41	0.56	0.58	0.92
Ni	T_C/T_C^{exp}	4.04	1.35	0.86	2.80	1.54
	θ_C/T_C^{exp}	4.03	1.34	0.90	2.78	1.60
	m_{eff}/m_{eff}^{exp}	0.85	0.64	0.86	0.81	1.51

Figure 2. The magnetization m/m_0 (——: calculation; ◆◆◆: experiment [25]), the mean square of the fluctuations of the on-site exchange field $\langle \Delta V_x^2 \rangle$ ($\cdot \cdot \cdot \cdot \cdot$) and $\langle \Delta V_z^2 \rangle$ (— — —) in units of the mean square of the exchange field at $T = 0$, the inverse paramagnetic susceptibility χ^{-1} (— $\cdot$ —) in units of $k_B T_C^{exp}/\mu_B^2$ and the local magnetic moment m_L/m_0 (— $\cdot \cdot$ —) of iron, calculated in the SLA as functions of the reduced temperature T/T_C.

Table 2. Experimental values of fundamental magnetic characteristics of iron, cobalt and nickel.

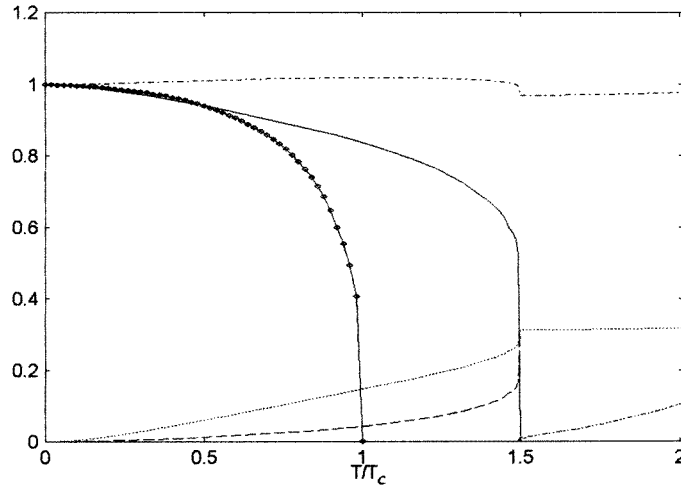|	Fe	Co	Ni
m_0 (μ_B) [25]	2.217	1.753	0.616
T_C^{exp} (K) [25]	1044.0	1390.0	631.0
m_{eff}^{exp} (μ_B) [26]	3.13	3.13	1.616

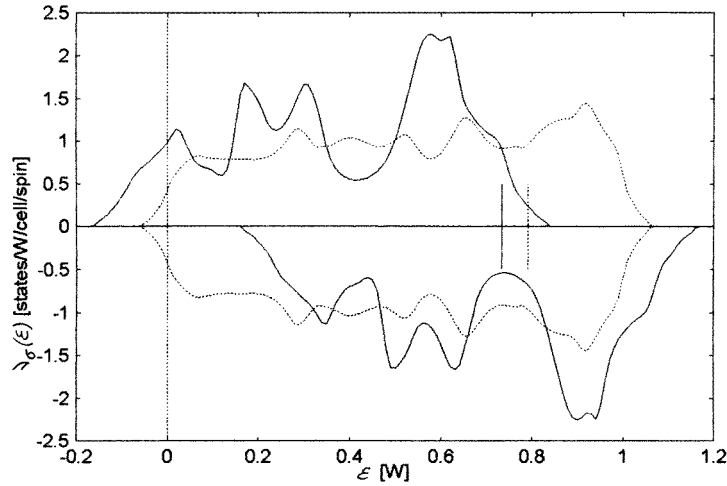**Figure 3.** As figure 2, but calculated in the DNA.

Figure 4. Spin-polarized DOSs of iron in the ferromagnetic ($T = 0$; solid curves) and paramagnetic ($T = 1.5T_C^{exp}$; dotted curves) states, calculated in the DNA. The vertical line indicates the position of the chemical potential μ.

Curie point Θ_C, obtained by the linear extrapolation of $\tilde{\chi}^{-1}(T)$ to zero, is nearly coincident with the ferromagnetic one.

In the static non-local approximation (SNA) the magnetization has to decrease faster than in the SLA. This is connected with the fact that the fluctuations ζ_{SN}^α are greater than the fluctuations ζ_{SL}^α at any temperature. Indeed, taking into account that $0 \leqslant \arctan(b/a) \leqslant \pi/2$, $0 \leqslant a^2 \leqslant 1$ and $b^2 = (1 - a^2)/0.6$, from formula (23) we have

$$\zeta_{SN}/\zeta_{SL} = \frac{3}{b^3}\left(b - a \arctan \frac{b}{a}\right) \geqslant \frac{3}{b^3}\left(b - a\frac{\pi}{2}\right) \geqslant \frac{3}{b^2} = \frac{3 \times 0.6}{1 - a^2} \geqslant 1.8.$$

As the calculations show, in the SNA the magnetization $m(T)$ decreases too fast.

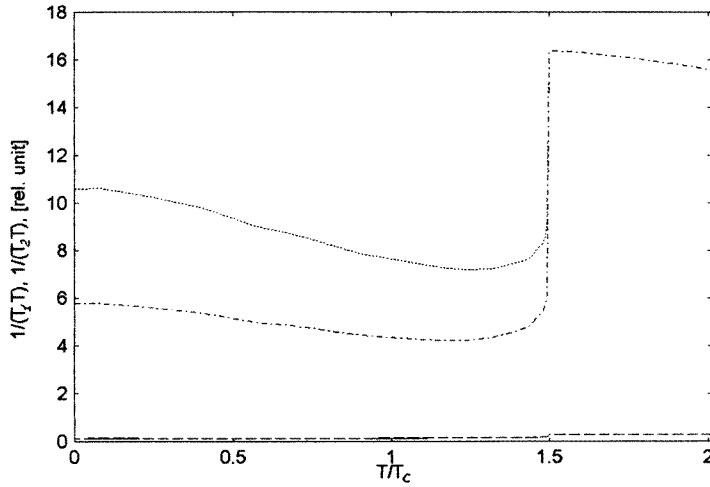In the dynamic local approximation (DLA) the fluctuations ζ_{DL}^α, calculated using

Figure 5. The temperature dependence of the longitudinal (T_1) and transverse (T_2) nuclear spin-relaxation times of iron, calculated in the DNA using the zero (——), (— — —) and enhanced ($\cdots\cdots$), (— $\cdot$ —) susceptibilities. (The solid curve coincides with the dashed one.)

formula (24), in contrast, are less than the fluctuations ζ_{SL}^{α} at any temperature ($\zeta_{DL}/\zeta_{SL} = (2/\pi)\arctan c \leqslant 1$). As the calculations show, in the DLA, $m(T)$ decreases too slowly.

Only in the dynamic non-local approximation (DNA) do the fluctuations ζ_{DN}^{α} with temperature increasing first increase slowly ($\sim T^2$), as in the DLA, and then increase quickly, as in the SNA. For this reason, at low temperatures the magnetization is proportional to T^2, which provides a good agreement with the experimental curve in the initial region (figure 3). At the same time, the Curie temperature T_C^{DN} obtained is equal to $1.49 T_C^{exp}$. The paramagnetic susceptibility follows the Curie–Weiss law, but the effective magnetic moment obtained is also a little greater than the experimental one: $m_{eff} = 1.3 m_{eff}^{exp}$. Figure 4 shows the mean DOSs $\nu_\sigma(\varepsilon, T)$ in the ferromagnetic ($T = 0$) and paramagnetic ($T = 1.5 T_C^{exp}$) states. In contrast to the mean-field-theory results, as the temperature increases, the functions $\nu_\uparrow(\varepsilon, T)$ and $\nu_\downarrow(\varepsilon, T)$, shifting toward each other, become noticeably smoothed. The nuclear spin-relaxation rates (figure 5) calculated without allowing for the enhancement depend only slightly on temperature, which is consistent with the known Korringa formula [27] for the relaxation time of the nuclear spin in simple metals. If the enhancement is taken into account, the values of $(T_1 T)^{-1}$ and $(T_2 T)^{-1}$ depend strongly on temperature, just as was observed experimentally in [28].

3.2. Cobalt

As the initial DOS, we take that of non-magnetic fcc cobalt from [24]. As for iron, the constant sp background was eliminated from it. After convoluting it with the Lorentz function of half-width $\Gamma = 0.01 W$ and normalizing it to one d band of unit width, we obtain the DOS represented in figure 6 by a solid curve. The bandwidth is $W = 7.50$ eV. The number of d electrons per atom obtained is equal to 8.47. The electron–electron interaction constant $u = 1.25$ eV is determined at $T = 0$ from the magnetic moment $m_0 = 1.45 \mu_B$. We are not able to find the constant u from the experimental value $m_0^{exp} = 1.753 \mu_B$ because for cobalt the magnetic moment m_0^{exp} is comparatively large and the Fermi energy is close to the band edge. To obtain m_0^{exp} it is necessary to move the DOSs $\nu_\uparrow(\varepsilon)$ and $\nu_\downarrow(\varepsilon)$ so far apart that the

sum $n_\uparrow + n_\downarrow$ becomes less than n_e. In our opinion, the discrepancy between $\nu(\varepsilon)$ and m_0^{exp} for cobalt is connected not with the fact that at $T = 0$ cobalt has hcp structure, because the DOS curves of hcp and fcc cobalt are very similar (see figure 5 in [26]), but rather with the fact that, in addition to the spin magnetic moment of the d electrons, m_0^{exp} includes the spin magnetic moment of the s electrons and the orbital magnetic moment, which, generally speaking, do not compensate for each other (see, e.g., [26, 29, 30]). The results of *ab initio* spin-polarized calculations of Fe, Co and Ni presented in [24, 31] also give evidence in favour of the chosen value $m_0 = 1.45 \, \mu_B$. If for iron and nickel the calculated spin magnetic moments m_0^{cal} are nearly the same as the experimental ones, then for fcc cobalt $m_0^{cal} = 1.54$–$1.56 \, \mu_B$. The value $m_0^{cal} = 1.56 \, \mu_B$ for fcc Co is also obtained in [32].
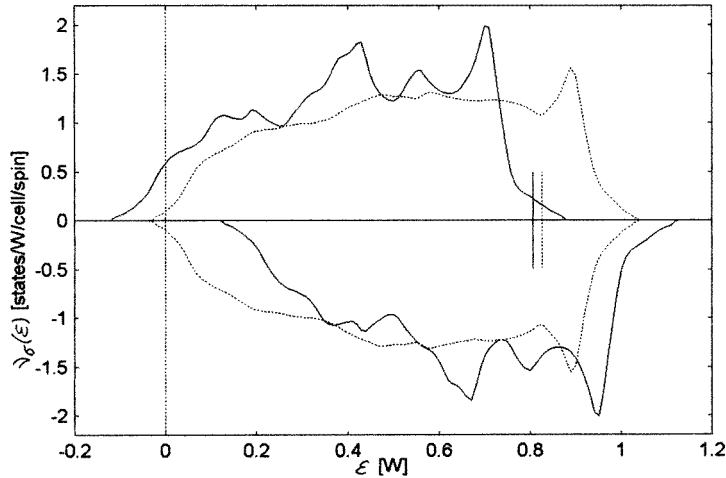

Figure 6. Spin-polarized DOSs of cobalt in the ferromagnetic ($T = 0$) and paramagnetic ($T = 0.64 T_C^{exp}$) states, calculated in the DNA. (The notation is as for figure 4.)

   The results of the calculations of the basic magnetic characteristics of cobalt within all of the above-mentioned approximations are listed in table 1. As for iron, the best ones are for DNA. As is seen from figure 7, at low temperatures the calculated magnetization $m(T)$ is in good agreement with the experimental one. The paramagnetic susceptibility satisfies the Curie–Weiss law with $m_{eff} = 0.92 m_{eff}^{exp}$. However, at high temperatures, $m(T)$ decreases too quickly and, as a consequence, $T = 0.63 T_C^{exp}$. On the whole, in spite of some discrepancies with experiment, the theoretical description of the magnetic properties of cobalt may be considered to be quite satisfactory.

   The mean DOSs $\nu_\sigma(\varepsilon, T)$ for the ferromagnetic ($T = 0$) and paramagnetic ($T = 0.64 T_C^{exp}$) states are shown in figure 6. As the temperature increases, the curves $\nu_\sigma(\varepsilon, T)$ behave as for iron, but are smoothed more noticeably.

3.3. Nickel

As for cobalt, the initial non-magnetic DOS was taken from [24]. After elimination of the sp background, convolution with the Lorentz function of half-width $\Gamma = 0.01W$ and normalization to one d band of unit width, the DOS represented in figure 8 by a solid curve was obtained. The bandwidth is $W = 6.13$ eV, and the number of d electrons per atom is $n_e = 9.35$. The electron–electron interaction constant $u = 1.16$ eV is determined from the
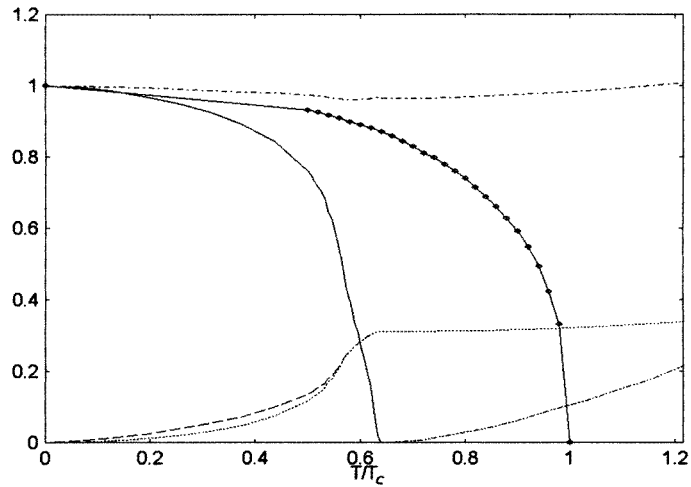
Figure 7. The magnetization m/m_0, the mean square of the fluctuations of the on-site exchange field $\langle \Delta V_x^2 \rangle$ and $\langle \Delta V_z^2 \rangle$, the inverse paramagnetic susceptibility χ^{-1} and the local magnetic moment m_L/m_0 of cobalt, calculated in the DNA. (The notation and units are as for figure 2.)
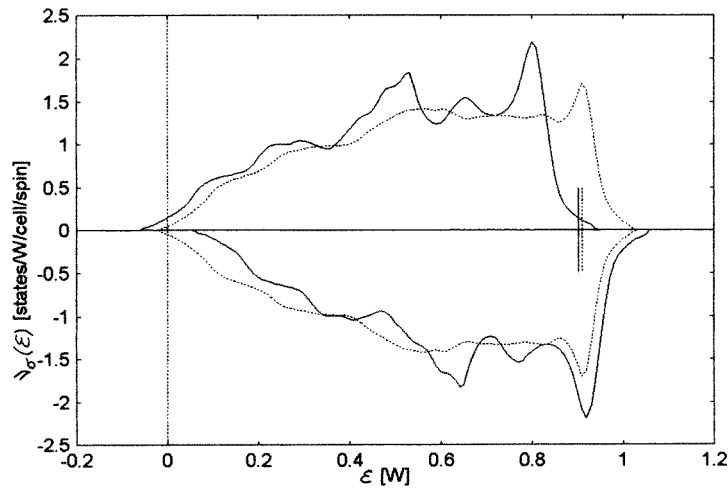

Figure 8. Spin-polarized DOSs of nickel in the ferromagnetic ($T = 0$) and paramagnetic ($T = 1.55 T_C^{exp}$) states, calculated in the DNA. (The notation is as for figure 4.)

experimental value of the magnetic moment of nickel $m_0^{exp} = 0.616 \, \mu_B$ [25].

The results of the calculations of the magnetic properties of nickel in various approaches are listed in table 1. The quantitative characteristics are similar to those for iron. On the whole, the best results are obtained in the DNA. As is seen from figure 9, in this approximation the spin fluctuations have the proper temperature behaviour and, as a consequence, the shape of the magnetization curve is in agreement with the experimental one. Note that in the ferromagnetic region, in iron the transverse fluctuations dominate, while in nickel the longitudinal fluctuations dominate and in cobalt the intermediate situation is realized: the transverse and longitudinal fluctuations are close in value (see figures 3, 7 and 9).

3.4. Comparison with the results of other work

Now let us compare our results with the results of recent work on calculations of the magnetic properties of Fe, Co and Ni [14–16, 20] that also used the real (not model) band structure. Some results of these studies are in better agreement with experiment than our results. However, good agreement, as a rule, is achieved only for some magnetic characteristics. In the paper [14], for all three metals a good agreement with experiment for the Curie temperature T_C is obtained. In the paper [15], for Fe good agreement with experiment is obtained for the Curie temperature: $T_C = 1015$ K, but not for the effective magnetic moment: $m_{eff} = 1.96 \, \mu_B$; for Ni, in contrast, the Curie temperature is almost one third smaller than the experimental one: $T_C = 450$ K, but the effective moment is fairly close to the experimental one: $m_{eff} = 1.21 \, \mu_B$. A similar situation is observed in the paper [16] too: the Curie temperature for Fe agrees well with experiment, whereas for Co and Ni there is a discrepancy of about 30%. Moreover, for all three metals the slope of the inverse paramagnetic susceptibility is almost twice as large as the experimental one. Finally, in the paper [20] a reasonable value of the Curie temperature for Ni has been obtained in the Stoner approximation with the usage, however, of additional experimental information. At the same time, the temperature behaviour of the calculated magnetization curve remained static-like. As for our results for the local magnetic moment in the paramagnetic region, they agree with the results of all of the above-mentioned spin-fluctuation calculations, except for those of [15], where the local moment of Ni above T_C appeared to be zero. Naturally, the same value of the local moment was obtained in the Stoner-like calculation in [20] too. However, as noted in the introduction, this result remains debatable.
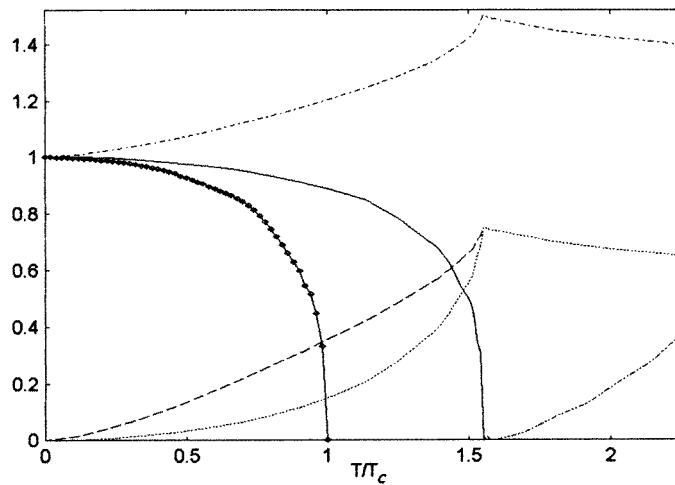

Figure 9. The magnetization m/m_0, the mean square of the fluctuations of the on-site exchange field $\langle \Delta V_x^2 \rangle$ and $\langle \Delta V_z^2 \rangle$, the inverse paramagnetic susceptibility χ^{-1} and the local magnetic moment m_L/m_0 of nickel, calculated in the DNA. (The notation and units are as for figure 2.)

From the DOS obtained in the band calculation, we eliminate the sp background and nonphysical sharp peaks. The sensitivity of the final results to these operations can be seen from comparison of our present results for Fe with those obtained in [13]. In the paper [13] the constant sp background was eliminated from the DOS given over the whole calculation interval, 15.2 eV. As a result, a DOS of width $W = 13.4$ eV was obtained, which was then smoothed out with $\Gamma = 0.01W = 0.134$ eV. In the present paper, the constant sp background

is eliminated from a DOS from which the fine extended 'tails' have already been cut off. (Of course, in both papers the remaining DOS is normalized to the total number of d states.) As a result, a DOS of width $W = 7.42$ eV and with $\Gamma = 0.01\,W = 0.0742$ eV is obtained, i.e. in the present paper the DOS is smoothed only half as much as in [13]. Consequently, the numerical values of several magnetic characteristics (T_C, Θ_C, m_{eff} etc) were somewhat changed, but the general temperature behaviour of all of the functions considered and the relation between the results of the calculations for various approximations of the SFT remained unchanged.

4. Conclusions

The numerical calculations for Fe, Co and Ni lend support to the validity of the method developed in [12, 13] for the description of the temperature dependence of the magnetic properties of ferromagnetic metals. From the four approximations of the SFT considered, the DNA turned out to be the best approximation for all three metals. The static approximation overestimates the contribution due to spin fluctuations and yields an incorrect temperature dependence of the magnetization and susceptibility (see figure 2). Only simultaneous consideration of the dynamics and non-locality (dependence on the wave vector) of the spin fluctuations ensures agreement of the theory with experiment. Note that the point in question is the proper (semiquantitative) description of the temperature behaviour of the magnetic properties on the whole. It is clear that in the framework of the approximations used for the electron–electron interaction (the Hubbard model, the single-site approximation etc), one should not expect quantitative coincidence—for example of T_C^{cal} with T_C^{exp}. So, electron–electron interaction beyond the LDA at zero temperature is characterized by just one constant, u, and the dependence of the magnetic properties upon u is fairly strong [33]. In the framework of the approximations used, one should also not expect a quantitative description of the temperature dependence of the magnetic properties in the critical region (see the theory for the critical region in, e.g., [34]).

Detailed investigations of local magnetic characteristics of Fe, Co and Ni, in particular the local magnetic moment and nuclear spin-relaxation times, (i) in the framework of the proposed approach and (ii) using the mean single-site Green function in the same manner as in [22], will be considered in a future paper.

Finally, note that in the alloys of ferromagnetic metals, which we intend to investigate in the future, the calculations by the proposed method will mostly be of predictive character. To carry out these calculations, one needs to know only the DOS and the magnetic moment at zero temperature.

Acknowledgment

Appendix. Calculation of the integrals involving the derivative of the Fermi function

Consider the integral

$$I = \int g(\varepsilon)\left(-\frac{\partial f(\varepsilon)}{\partial \varepsilon}\right)\,\mathrm{d}\varepsilon \tag{A.1}$$

where $g(\varepsilon)$ is an arbitrary function, vanishing for $\varepsilon \to \pm\infty$, and $f(\varepsilon)$ is the Fermi function. Let us represent the function $f(\varepsilon)$ as a sum of the step function

$$\Theta(\varepsilon - \mu) = \begin{cases} 1 & \text{when } \varepsilon < \mu \\ 1/2 & \text{when } \varepsilon = \mu \\ 0 & \text{when } \varepsilon > \mu \end{cases}$$

and the function

$$f_2(\varepsilon) = \text{sgn}(\varepsilon - \mu) \left[e^{|\varepsilon - \mu|/T} + 1 \right]^{-1} = -T \frac{\partial}{\partial \varepsilon} \ln(1 + e^{-|\varepsilon - \mu|/T}). \tag{A.2}$$

Substituting $f(\varepsilon) = \Theta(\varepsilon - \mu) + f_2(\varepsilon)$ into (A.1), we split the integral I into two integrals:

$$I = \int g(\varepsilon) \left(-\frac{\partial \Theta(\varepsilon - \mu)}{\partial \varepsilon} \right) \mathrm{d}\varepsilon + \int g(\varepsilon) \left(-\frac{\partial f_2(\varepsilon)}{\partial \varepsilon} \right) \mathrm{d}\varepsilon \equiv I_1 + I_2.$$

For the first integral we immediately obtain

$$I_1 = \int g(\varepsilon)\delta(\varepsilon - \mu) \, \mathrm{d}\varepsilon = g(\mu). \tag{A.3}$$

For the second one we first use integration by parts:

$$I_2 = \int \frac{\partial g(\varepsilon)}{\partial \varepsilon} f_2(\varepsilon) \, \mathrm{d}\varepsilon. \tag{A.4}$$

Then, using a linear interpolation, we transform the tabular function $g(\varepsilon)$ into a piecewise-linear function:

$$g(\varepsilon) = \begin{cases} a_i(\varepsilon - \varepsilon_i) + b_i & \varepsilon_i \leqslant \varepsilon \leqslant \varepsilon_{i+1} \\ 0 & \varepsilon < \varepsilon_1 \text{ and } \varepsilon > \varepsilon_{n+1} \end{cases} \tag{A.5}$$

where $a_i = (b_{i+1} - b_i)/(\varepsilon_{i+1} - \varepsilon_i)$, $b_i = g(\varepsilon_i)$, $i = 1, \ldots, n + 1$, and n is the number of intervals. The substitution of (A.5) and (A.2) into (A.4) yields

$$I_2 = \sum_{i=1}^{n} a_i \int_{\varepsilon_i}^{\varepsilon_{i+1}} f_2(\varepsilon) \, \mathrm{d}\varepsilon = T \sum_{i=1}^{n} a_i \left[\ln(1 + e^{-|\varepsilon_i - \mu|/T}) - \ln(1 + e^{-|\varepsilon_{i+1} - \mu|/T}) \right]. \tag{A.6}$$

Taking into account (A.3) and (A.6), for the initial integral (A.1) we obtain

$$I = g(\mu) + T \sum_{i}' a_i \left[\ln(1 + e^{-|\varepsilon_i - \mu|/T}) - \ln(1 + e^{-|\varepsilon_{i+1} - \mu|/T}) \right]. \tag{A.7}$$

The prime indicates that the sum includes only those terms for which $|\varepsilon_i - \mu| \leqslant t \ln \beta T$, where β is the base and t the precision of the floating-point system of the specific computer (see, e.g., [35]).

References

[1] Stoner E C 1938 *Proc. R. Soc.* A **165** 372
[2] Moriya T 1985 *Spin Fluctuations in Itinerant Electron Magnetism* (Berlin: Springer)
[3] Capellmann H (ed) 1987 *Metallic Magnetism* (Berlin: Springer)
[4] Hubbard J 1979 *Phys. Rev.* B **19** 2626
     Hubbard J 1979 *Phys. Rev.* B **20** 4584
[5] Hasegawa H 1979 *J. Phys. Soc. Japan* **46** 1504
     Hasegawa H 1980 *J. Phys. Soc. Japan* **49** 178
     Hasegawa H 1980 *J. Phys. Soc. Japan* **49** 963
[6] Hubbard J 1981 *Phys. Rev.* B **23** 5974
[7] Kakehashi Y 1981 *J. Phys. Soc. Japan* **50** 2251
[8] Grebennikov V I, Prokopjev Yu I, Sokolov O B and Turov E A 1981 *Phys. Met. Metallogr.* **52** 1

[9] Kakehashi Y and Fulde P 1985 *Phys. Rev.* B **32** 1595
[10] Kakehashi Y 1986 *Phys. Rev.* B **34** 3243
[11] Shi F-j and Lin T-h 1993 *Phys. Rev.* B **48** 12 795
[12] Reser B I and Grebennikov V I 1997 *Phys. Met. Metallogr.* **83** 127
[13] Reser B I and Grebennikov V I 1998 *Phys. Met. Metallogr.* **85** 20
[14] Mohn P and Wohlfarth E P 1987 *J. Phys. F: Met. Phys.* **17** 2421
[15] Staunton J B and Gyorffy B L 1992 *Phys. Rev. Lett.* **69** 371
[16] Uhl M and Kübler J 1996 *Phys. Rev. Lett.* **77** 334
[17] Murata K K and Doniach S 1972 *Phys. Rev. Lett.* **29** 285
[18] Lonzarich G G and Taillefer L 1985 *J. Phys. C: Solid State Phys.* **18** 4339
[19] Brout R and Thomas H 1967 *Physics* **3** 317
[20] Basalis N C, Theodorakopoulos N and Papaconstantopoulos D A 1997 *Phys. Rev.* B **55** 11 391
[21] Grebennikov V I, Kuznetsov V L and Sokolov O B 1992 *Sov. Phys.–Solid State* **34** 681
[22] Reser B I and Prokopjev Yu I 1992 *Phys. Met. Metallogr.* **74** 123
     Reser B I 1994 *Phys. Met. Metallogr.* **77** 451
[23] Reser B I 1996 *J. Phys.: Condens. Matter* **8** 3151
[24] Moruzzi V L, Janak J F and Williams A R 1978 *Calculated Electronic Properties of Metals* (New York: Pergamon)
[25] Crangle J and Goodman G M 1971 *Proc. R. Soc.* A **321** 477
[26] Wohlfarth E P 1980 *Ferromagnetic Materials* vol 1, ed E P Wohlfarth (Amsterdam: North-Holland)
[27] Korringa J 1950 *Physica* **16** 601
[28] Shaham M, Barak J, El-Hanany U and Warren W W Jr 1980 *Phys. Rev.* B **22** 5400
[29] *Landolt–Börnstein New Series* 1987 Group III, vol 19a (Berlin: Springer)
[30] Eriksson O, Johansson B, Albers R C and Boring A M 1990 *Phys. Rev.* B **42** 2707
[31] Sandratskii L M and Kübler J 1992 *J. Phys.: Condens. Matter* **4** 6927
[32] Moruzzi V L, Markus P M, Schwarz K and Mohn P 1986 *J. Magn. Magn. Mater.* **54–57** 955
[33] Prokopjev Yu I and Reser B I 1991 *J. Phys.: Condens. Matter* **3** 6055
[34] Hertz J A 1971 *Int. J. Magn.* **1** 253
[35] Forsythe G E, Malcolm M A and Moler C B 1977 *Computer Methods for Mathematical Computations* (Englewood Cliffs, NJ: Prentice-Hall)